Thermodynamic activation parameters in the fluxional behavior of CH2[(.eta.5-C5H4)M(CO)]2(.mu.-CO), where M = rhodium or iridium. Crystal structure of CH2[(.eta.5-C5H4)Ir(CO)]2(.mu.-CO)

Thomas E. Bitterwolf, Alessandro. Gambaro, Francesca. Gottardi, and Giovanni. Valle

Organometallics, **1991**, 10 (5), 1416-1420• DOI: 10.1021/om00051a037 • Publication Date (Web): 01 May 2002

mined in the presence of 1 equiv of THF within experimental error.

Thermolyses in the presence of $[^nBu_4N][BPh_4]$ (0.07–0.16 M) were carried out at 30.5 ± 0.5 °C in the NMR probe, due to the poor solubility of $[^nBu_4N][BPh_4]$ at low temperature.

Calibration of Gas Bulb. To check the accuracy of the $[CD_3CN]$ measurement described above, solutions of CH_3CN in CD_2Cl_2 were prepared by gas bulb measurements and $[CH_3CN]$ was determined by the ideal gas law and by ^1H NMR integration relative to an internal standard. Bibenzyl and ferrocene were used as the standard in separate experiments. For each of three gas bulbs used in this work (volume 489.4, 214.4, 109.9 mL; pressure 60–70 mmHg), five independently prepared samples showed $[CH_3CN]_{calc}/[CH_3CN]_{obs} = 1.00 \pm 0.10$. In addition, the amount of CH_3CN added was calculated by the van der Waals equation $(P + n^2a/V^2)(V - nb) = nRT$ (where $a = 17.58$ L²·atm·mol^{-2} and $b = 0.1168$ L·mol).[52] The calculated n from this equation showed ≤0.5% deviation from that of the ideal gas law. Thus, deviation from ideal gas behavior is negligible under these conditions.

Determination of K_{eq} by NMR Spectroscopy. The K_{eq} value for eq 5 at 30 °C for **7** and **10** was determined from the variation of $\delta(Zr-CH_3)$ (^1H NMR) vs $[CD_3CN]$ by assuming that the solvent effect on the chemical shift is minimal and δ_{mono} = 0.68 for **6** and 0.59 for **9**. Solutions of **6** or **9** in CD_2Cl_2 containing CD_3CN were prepared as described above. The ^1H NMR spectrum at 30 °C was recorded for each sample: $\delta(Zr-CH_3)_{obs}$ ($[CD_3CN]$, M) 0.14 (0.51), 0.13 (0.97), 0.12 (2.07), and 0.11 (3.07) for **6**; $\delta(Zr-CH_3)_{obs}$ ($[CH_3CN]$, M) 0.12 (0.97), 0.13 (0.99), 0.05 (3.36), and 0.05 (3.87) for **9**. For each compound a plot of $\delta(Zr-CH_3)_{obs}$ vs $(\delta_{mono} - \delta_{obs})/[CD_3CN]$ was linear. The slope of the plot equals K_{eq} (0.036 (5) M for **6** and 0.23 (2) M for **9**), and the intercept of the plot equals δ_{bis} (0.11 for **6** and 0.02 for **9**).[53]

Determination of $E_T(30)$ Values of CH_3CN/CH_2Cl_2 Mixed Solvents. The $E_T(30)$ values for CH_3CN/CH_2Cl_2 mixed solvents were determined with use of the literature procedure.[54] UV-visible spectra of Reichardt's dye in CH_2Cl_2 solutions containing 1.0, 1.5, 2.0, 2.5, 3.0, 3.5, 4.0, and 4.5 M of CH_3CN were recorded. For each solution $E_T(30)$ was determined according to the equation $E_T(30) = (28\,590 \text{ kcal·nm})/\lambda_{max}$. These data were fit to the equation $E_T(30) = E_D \ln([CD_3CN]/Cp^* + 1) + E_T^0(30)$, where $E_T^0(30)$ is the $E_T(30)$ value in neat CH_2Cl_2 (40.7 kcal/mol). The unknown parameters Cp^* and E_D were determined by nonlinear least-squares analysis ($Cp^* = 5.17$ (52), $E_D = 3.38$ (34)). A plot of $E_T(30)$ vs $\ln([CH_3CN]/Cp^* + 1)$ produced a straight line ($R = 0.995$), from which $E_T(30)$ values for other $[CD_3CN]$ were determined.

Acknowledgment. Early portions of this work were performed at Washington State University. We are in debt to Dr. Dennis Taylor for his generous supply of complex **6**. This work was supported by NSF Grant CHE8816445 and by DOE Grant DE-FG02-88ER13935. R.F.J. gratefully acknowledges a Sloan Foundation Research Fellowship (1989–1991) and Union Carbide Research Innovation Awards (1989, 1990).

(52) *CRC Handbook of Chemistry and Physics*, 60th ed.; CRC: Boca Raton, FL, p D-194.

(53) Drago, R. S. *Physical Methods in Chemistry*; W. B. Saunders: Philadelphia, PA, 1977; p 252.

(54) Langhals, H. *Tetrahedron Lett.* **1986**, *27*, 339.

Thermodynamic Activation Parameters in the Fluxional Behavior of $CH_2[(\eta^5\text{-}C_5H_4)M(CO)]_2(\mu\text{-}CO)$, Where M = Rh or Ir. Crystal Structure of $CH_2[(\eta^5\text{-}C_5H_4)Ir(CO)]_2(\mu\text{-}CO)$

Thomas E. Bitterwolf*

Department of Chemistry, University of Idaho, Moscow, Idaho 83843

Alessandro Gambaro and Francesca Gottardi

Department of Physical Chemistry, University of Padova, via Loredan 2, 35131 Padova, Italy

Giovanni Valle

CNR, Centro di Studio sui Biopolimeri, Department of Organic Chemistry, University of Padova, via Marzolo 3, 35131 Padova, Italy

Received November 14, 1990

The synthesis and molecular structure of $CH_2[(\eta^5\text{-}C_5H_4)Ir(CO)]_2(\mu\text{-}CO)$ is reported. ^{13}CO enrichment of the analogous rhodium complex, $CH_2[(\eta^5\text{-}C_5H_4)Rh(CO)]_2(\mu\text{-}CO)$, is also reported. Variable-temperature ^1H NMR studies of $CH_2[(\eta^5\text{-}C_5H_4)Ir(CO)]_2(\mu\text{-}CO)$ and corresponding ^1H and ^{13}C NMR studies of its rhodium analogue have been carried out. The low-temperature limiting spectra of both compounds have been fully analyzed. Coalescence temperatures for each of the three pairs of exchanging protons for the Rh and Ir complexes have been recorded, and the coalescence temperatures for the carbonyls in the rhodium compound have been recorded. Calculated $\Delta G^\ddagger$ values for the rhodium complex support a mechanism in which the ring and carbonyl motions are coupled. Comparison of $\Delta G^\ddagger$ values for the rhodium and iridium complexes reveals a substantially higher barrier for the iridium compound than for the rhodium.

The fluxional motions of a large number of dinuclear cyclopentadienyl metal carbonyl compounds have been studied in which the interconversion of cis and trans rotamers has been proposed to occur through a sequence of carbonyl bridge openings and subsequent rotations.[1] Similarly, the site exchange of terminal and bridging carbonyl groups of *trans*-$Cp_2Rh_2(CO)_2L$, where L = CO or PPh_3, has been studied by variable-temperature ^{13}C NMR, and mechanisms involving two or three bridging carbonyl groups in the exchange intermediate have been proposed.[2,3]

(1) Cotton, F. A.; Wilkinson, G. *Advanced Inorganic Chemistry*, 5th ed.; J. Wiley and Sons: New York, **1988**; p 1325.

(2) (a) Evans, J.; Johnson, B. F. G.; Lewis, J.; Norton, J. R. *J. Chem. Soc., Chem. Comm.* **1973**, 79. (b) Evans, J.; Johnson, B. F. G.; Lewis, J.; Matheson, T. W.; Norton, J. R. *J. Chem. Soc., Dalton Trans.* **1978**, 626.

0276-7333/91/2310-1416$02.50/0

Table I. Crystal Data, Details of Intensity Data, and Structure Refinement of II

mol wt	610.4
system	orthorhombic
space group	*Pcmn* (No. 62)
cell constants	
a, Å	6.150 (1)
b, Å	13.957 (2)
c, Å	14.711 (2)
cell vol, Å^3	1262.7
Z	4
ρ(calcd), g cm^{-3}	3.221
ρ(meas), g cm^{-3}	3.20
radiation	Mo Kα (0.7107 Å)
cryst dimens, mm	0.2 × 0.2 × 0.4
μ, cm^{-1}	32.2
2θ range, deg	50°
decay of std rflns	±2%
no. of rflns collected	1586
no. of unique rflns	1586
no. of rflns obsd	1239
R_{factor}	0.081

Several examples of dinuclear cyclopentadienyl metal carbonyl compounds in which the two cyclopentadienyl rings are coupled by alkyl groups are now known.[4,5] Werner et al.[5] have reported the molecular structure of $CH_2[(\eta^5\text{-}C_5H_4)Rh(CO)]_2(\mu\text{-}CO)$, I in which the molecule possesses a mirror plane of symmetry passing through the methylene bridge, the midpoint of the Rh–Rh bond, and the μ-CO. In the solid state the two methylene hydrogens are in different environments, and the protons of the cyclopentadienyl rings occupy four different environments. Substitution of the μ-CO with a μ-CH_2 gives a molecular species whose solid-state structure is isomorphous with that of I.[6]

The room-temperature ^{1}H NMR spectrum of I has been reported[4a,5] and consists of an ill-resolved AA′BB′ pattern for the cyclopentadienyl ring protons and a singlet for the methylene group. Such a spectrum would imply that the molecule undergoes a rapid fluxional movement in which methylene bridge and cyclopentadienyl ring proton environments are being averaged.

We have now prepared $CH_2[(\eta^5\text{-}C_5H_4)Ir(CO)]_2(\mu\text{-}CO)$, II, the iridium analogue of I, and have found that its room-temperature ^{1}H NMR spectrum consists of a set of four, ill-resolved multiplets for the cyclopentadienyl ring hydrogens and an AB pattern for the methylene group. This is the pattern that would be expected if the molecule were either rigid, or undergoing an exchange which is slow on the NMR time scale. The unexpected observation of substantially different thermal barriers between the rhodium and iridium compounds prompted us to initiate a detailed variable-temperature analysis of the dynamic behaviors of I and II. The resulting $\Delta G^{\ddagger}$ values obtained from these studies are discussed in connection with the possible mechanisms of the interconversion process, as well as the influence of the bridge and metal on the barrier to exchange.

Results and Discussion

We have previously reported that $CH_2[(\eta^5\text{-}C_5H_4)Rh(CO)_2]_2$ readily loses carbon monoxide in refluxing benzene to give the μ-CO derivative, I, but that $CH_2[(\eta^5\text{-}C_5H_4)Ir(CO)_2]_2$ is inert to carbon monoxide loss under these conditions.[4a] Pierpont and his co-workers[7] have reported that $(\eta^5\text{-}C_5H_5)Ir(CO)_2$ can be converted to $[(\eta^5\text{-}C_5H_5)Ir(CO)]_2(\mu\text{-}CO)$ by reflux with trimethylene oxide in benzene. Similarly, we have found that $CH_2[(\eta^5\text{-}C_5H_4)Ir(CO)_2]_2$ can be converted to $CH_2[(\eta^5\text{-}C_5H_4)Ir(CO)]_2(\mu\text{-}CO)$, II, in the same manner. II is recovered in good yield as an air-stable, orange microcrystalline powder. The infrared spectrum of II contains two bands in the terminal carbonyl region and one band in the bridging carbonyl region. The terminal bands have a "strong–weak" intensity pattern which is identical with that observed for I and is characteristic

Table II. Final Positional Parameters with Standard Deviations in Parentheses (×10^4) for II

atom	*x*/*a*	*y*/*b*	*z*/*c*
Ir	1944 (2)	1546 (1)	738 (1)
O(1)	-113 (64)	2500	-896 (28)
O(2)	5358 (52)	1165 (24)	-649 (29)
C(1)	743 (79)	2500	-158 (27)
C(2)	3908 (85)	1315 (26)	-147 (24)
C(3)	-1440 (80)	2500	2248 (42)
C(4)	-221 (51)	1603 (29)	1977 (20)
C(5)	1878 (60)	1326 (23)	2274 (24)
C(6)	2331 (62)	427 (25)	1830 (22)
C(7)	517 (67)	158 (22)	1278 (24)
C(8)	-1074 (58)	868 (28)	1369 (24)

Table III. Selected Geometrical Parameters for II[a]

Bond Lengths and Nonbonded Distances, Å

Ir–Ir*	2.664 (2)	C1–O1	1.207 (58)
Ir–C1	2.014 (31)	C2–O2	1.177 (59)
Ir–C2	1.805 (44)	C3–C4	1.512 (48)
Ir–C4	2.258 (31)	C4–C5	1.417 (48)
Ir–C5	2.281 (35)	C5–C6	1.441 (48)
Ir–C6	2.253 (34)	C6–C7	1.430 (53)
Ir–C7	2.269 (33)	C7–C8	1.399 (52)
Ir–C8	2.280 (37)	C8–C9	1.458 (52)
Ir–M	1.915 (36)		

Bond Angles, deg

Ir–C1–Ir*	82.8 (1.6)	M–Ir–C2	137.8 (1.3)
Ir–C1–O1	138.5 (0.8)	C4–C3–C4*	111.7 (4.2)
Ir–C2–O2	172.6 (4.0)	C4–C5–C6	105.9 (3.1)
C1–Ir–Ir*	48.6 (0.9)	C5–C6–C7	109.6 (3.1)
C1–Ir–C2	83.7 (1.8)	C6–C7–C8	107.8 (2.9)
C2–Ir–Ir*	100.3 (1.2)	C7–C8–C4	107.8 (3.1)
M–Ir–Ir*	119.2 (1.0)	C8–C4–C5	108.9 (3.2)
M–Ir–C1	132.9 (2.0)	C3–C4–C8	124.5 (3.2)

Interplanar Angles, deg

M–Ir–Ir*–M*/Ir–C1–O1–Ir*	124.5
M–Ir–Ir*–M*/Ir–C2–O2–Ir*	161.9
M–Ir–Ir*–M*/C4–C3–C4*	34.4
Ir–C1–O1–Ir*/Ir–C2–O2–Ir*	73.6
C4 to C8/C4* to C8*	121.6

Distances of C1–C8, O1, and O2 Atoms from the Plane M–Ir–Ir*–M*, Å

C1	1.265	C8	1.216
O1	2.234	C2	-0.468
C3	0.817	O2	-0.917
C4	0.337	C5	-1.009
C7	0.411	C6	-0.954

Distances of C4–C8 Atoms from the Plane O1–C1–C3, Å

C4	1.252	C7	3.269
C5	1.638	C8	2.278
C6	2.894		

[a] M represents the baricenter of cyclopentadienil rings. The asterisks (*) indicate the atoms of the symmetric part of the molecule.

(3) Adams, R. D.; Brice, M. D.; Cotton, F. A. *Inorg. Chem.* **1974**, *13*, 1080.
(4) (a) Bitterwolf, T. E. *J. Organometal. Chem.* **1986**, *312*, 197. (b) Bitterwolf, T. E. *J. Organometal. Chem.* **1990**, *386*, 9. (c) Bitterwolf, T. E., Horine, P.; Rheingold, A. L. Unpublished results.
(5) Werner, H.; Scholz, J. J.; Zolk, R. *Chem. Ber.* **1985**, *118*, 4531.
(6) Bitterwolf, T. E.; Rheingold, A. L. *Organometallics* **1987**, *6*, 2138.
(7) Shapley, J. R.; Adair, P. C.; Lawson, R. J.; Pierpont, C. G. *Inorg. Chem.* **1982**, *21*, 1701.

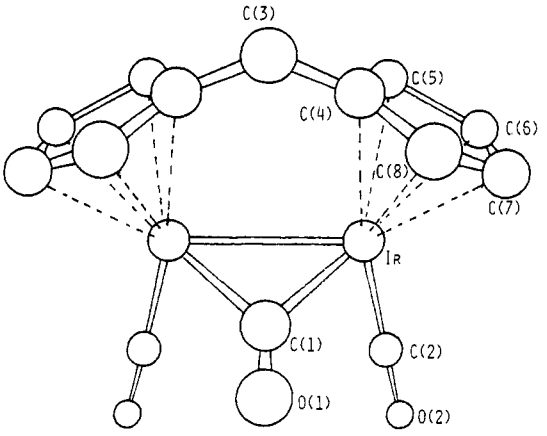

Figure 1. Molecular structure of II.

of a cis molecular orientation.

X-ray quality crystals of II were obtained from solutions of II in dichloromethane which were stored in a freezer for about 2 weeks. Crystal data, intensity, and refinement data are presented in Table I. Final atom position parameters are presented in Table II. Design limitations on the diffractometer prevented the collection of data at $2\theta < 45°$, thus refinement of the molecular structure below 8% was not possible. Recognizing these limitations, it is clear that the structure of II (Figure 1) is isomorphous with that previously reported for I[5] and that, with minor differences in bond lengths and angles, and two structures are almost superimposable. Table III presents selected bond lengths and angles for II. We have adopted the atomic numbering pattern used by Werner et al.[5] for the structure of I to simplify comparison of the two structures.

Examination of the crystal structures of I, II, CH_2-$[(\eta^5\text{-}C_5H_4)Rh(CO)]_2(\mu\text{-}CH_2)$,[6] and the recently prepared $C_2H_4[(\eta^5\text{-}C_5H_4)Rh(CO)]_2(\mu\text{-}CO)$[4c] reveals that the bridges connecting the rings are found on the same side of the molecule as the μ-CO or μ-CH_2 group.

Variable-temperature NMR studies were carried out on solutions of I in CD_2Cl_2 (^{1}H, 80 MHz) and $CDCl_3$ (^{1}H, 300 MHz and ^{13}C, 75 MHz), and II in $C_2D_2Cl_4$ (^{1}H, 80 MHz). A partial study of II was also conducted in CD_2Cl_2 (^{1}H, 80 MHz), but was limited to a maximum of 50.5 °C because of the formation of vapor bubbles in the solvent. The solvents were selected on the basis of compound solubility and required thermal ranges. It was also believed that the intermolecular forces of these solvents were sufficiently similar that solvent effects on the resulting thermodynamic parameters would be minimized. Small amounts of decomposition of II were observed after measurement of the high-temperature spectra, but this decomposition did not alter the appearance of the spectrum.

Detailed analysis of the low-temperature limiting ^{1}H NMR spectra of I and II were carried out. The low-temperature limiting spectrum of I is presented in Figure 2a. These results are summarized in Table IV. Both compounds exhibit unique ABCD patterns for the cyclopentadienyl rings and AB patterns for the methylene group coupling the rings. In I, small two- and three-bond coupling between the rhodium atoms and the H-C_6 and H-C_7 protons were observed. The ring protons H-C_5 and H-C_8 couple with the methylene protons.

Increasing the temperature from low-temperature limits permitted the coalescence temperatures, T_c, of the methylene protons, the H-C_6 and H-C_7 protons, and the H-C_5 and the H-C_8 protons to be observed. In the ranges of proton coalescence, 80-MHz spectra were recorded at 1 °C intervals to provide a high reliability to the assigned coalescence temperatures. Studies done on I at 300 MHz were focused on the ^{13}C spectra and were recorded at 5 °C intervals. The observed coalescence temperatures and

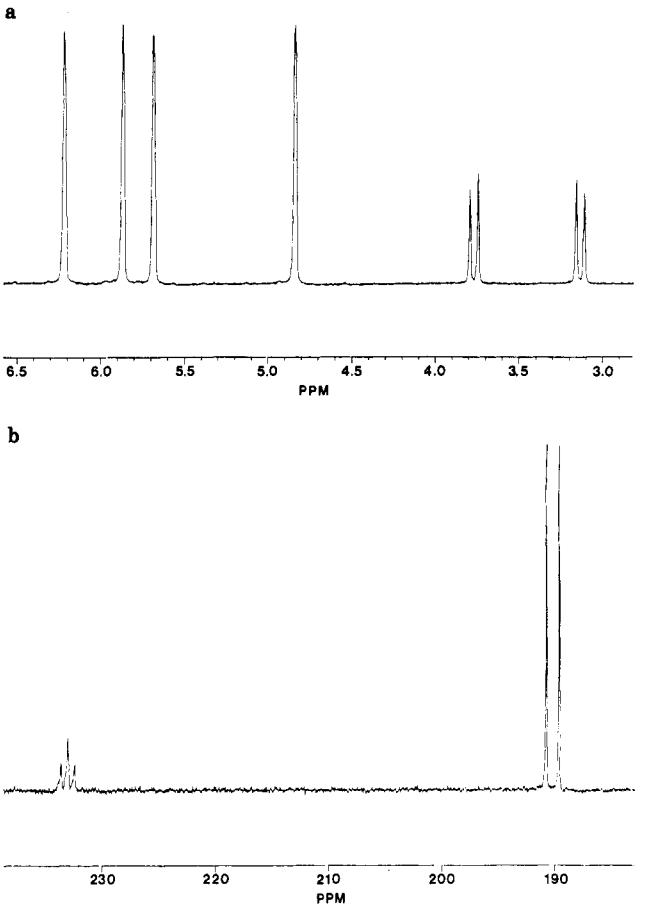

Figure 2. (a) Low-temperature ^{1}H NMR spectrum of I in $CDCl_3$ at 240 K. (b) Low-temperature ^{13}C NMR spectrum of the carbonyl region of I in $CDCl_3$ at 240 K.

Table IV. ^{1}H NMR Parameters for I and II

	chemical shifts,[e] ppm		
H_i[d]	I[a]	II[b]	II[c]
3a	3.874	4.260	4.275
3b	3.329	3.989	4.174
5	6.149	6.095	6.047
6	5.904	5.933	5.928
7	5.730	5.624	5.621
8	4.841	4.742	4.739
	coupling constants,[f,g] Hz		
i,j	I[a]	II[b]	II[c]
3a,3b	−14.40 ± 0.01	−14.50 ± 0.03	−14.36 ± 0.05
3a,5	0.60 ± 0.01	0.4[h]	0.41 ± 0.06
3a,8	0.44 ± 0.01	0.3[h]	0.40 ± 0.07
3b,5	0.66 ± 0.02	0.4[h]	0.44 ± 0.06
3b,8	0.47 ± 0.01	0.3[h]	0.36 ± 0.07
5,6	3.00 ± 0.01	2.65 ± 0.02	2.61 ± 0.03
5,7	1.58 ± 0.02	1.53 ± 0.03	1.55 ± 0.03
5,8	1.60 ± 0.01	1.54 ± 0.03	1.55 ± 0.03
6,7	2.34 ± 0.02	2.52 ± 0.02	2.57 ± 0.04
6,8	1.58 ± 0.01	1.47 ± 0.02	1.51 ± 0.04
7,8	2.92 ± 0.02	2.69 ± 0.03	2.67 ± 0.04

[a] T = −54.7 °C, solvent CD_2Cl_2. [b] T = −1.9 °C, solvent $CDCl_2$–$CDCl_2$. [c] T = −1.0 °C, solvent CD_2Cl_2. [d] Proton labelling is that of the X-ray structure (Figure 1), H_{3b} is the methylene proton that points toward the same direction of μ-CO; this assignment parallels that for $CH_2[(\eta^5\text{-}C_5H_4)Rh(CO)]_2\text{-}(\mu\text{-}CH_2)$. [e] Ppm from internal TMS, error ± 0.001 ppm. [f] Coupling constants of methylene protons with H_6 and H_7 are less than 0.2 Hz. [g] ^2J(Rh, H_2) = −0.39 ± 0.03, ^3J(Rh, H_2) ≲ 0.1, ^2J(Rh, H_3) = 0.79 ± 0.02, ^3J(Rh, H_3) = 0.78 ± 0.02, Hz. [h] Not refined by iteration.

Table V. Thermodynamic Parameters for I and II

	I			II		
H_iH_j	$\Delta\nu$, Hz	T_c, K	$\Delta G^{\ddagger}$, kJ/mol	$\Delta\nu$, Hz	T_c, K	$\Delta G^{\ddagger}$, kJ/mol
3a,3b	43.68[a]	265	54.5	21.76[c]	329	70.2
	191.04[b]	280	54.3			
5,8	104.76[a]	275	54.7	108.41[c]	360	72.3
	414.49[b]	285	53.5			
6,7	13.98[a]	252	54.1	24.69[c]	331	70.3
	54.44[b]	275	56.2			
CO	3296[b]	315	54.3, 56.1			

[a] CD_2Cl_2, 80-MHz NMR. [b] $CDCl_3$, 300-MHz NMR. [c] $C_2D_2Cl_4$, 80-MHz NMR.

calculated values for $\Delta G^{\ddagger}$ are reported in Table V.

^{13}C spectra (300 MHz) were recorded on a ^{13}CO-enriched sample of I prepared as described in the Experimental Section. The low-temperature limiting spectrum of the carbonyl region of I is presented in Figure 2b. In the low-temperature limiting spectrum, the bridging carbonyl is split into a triplet and the terminal carbonyls into a doublet by the 100% abundant rhodium nuclei (spin = $^1/_2$). A small additional splitting of the bridging carbonyl resonance is probably attributable to a small amount of double labeled material in which a bridging carbonyl is coupling to a ^{13}C in a terminal carbonyl. The ring carbons appear as separate resonances, but no effort was made to attempt to assign these resonances. Increasing the temperature from the low-temperature limit in 5 °C intervals resulted in the observation of T_c of the carbonyl carbons. The resonances for the ring carbons also coalesced giving two closely spaced resonances at their high-temperature limit.

Calculations of $\Delta G^{\ddagger}$ values for the various exchange processes occurring in these compounds require that considerable assumptions be made which simplify the computations. Exchange of the ring proton pairs H-C_5, H-C_8 and H-C_6, H-C_7 can be treated as simple uncoupled, two site exchanges so that the conventional rate expression

$$k = \pi\delta\nu/\sqrt{2} \qquad (1)$$

can be used without correction. Exchange of the methylene protons, and the carbonyl carbons, however, involves either coupled atoms or unequal populations, both of which require that additional assumptions be made. Kost, Carlson, and Raban have demonstrated that coupled AB systems can be approximated by the expression[8]

$$k = (\pi/\sqrt{2})[(\delta\nu)^2 + 6J^2]^{1/2} \qquad (2)$$

For $\delta\nu/J > 3$ eq 1 gives acceptable approximations, and in the present case $\delta\nu/J > 13$, thus both eqs 1 and 2 give similar results for k. Exchange of unequal populations such as the carbonyls can be addressed by using the techniques developed by Shanan-Atidi and Bar-Eli,[9] as employed by Lewis et al. in their study of $[(\eta^5\text{-}C_5H_5)Rh(CO)]_2(\mu\text{-}CO)$.[2] In the present case, these values of the rate constant k are being used to calculate approximate values for $\Delta G^{\ddagger}$ by using T_c such that the errors in k are less important than errors in T_c.[10]

Several conclusions can be drawn from the available data. $\Delta G^{\ddagger}$ values for I and II were each obtained in two different, although closely related, solvents. Within the limits of experimental error, there was no significant influence of solvent on the $\Delta G^{\ddagger}$ values for the fluxional motions.

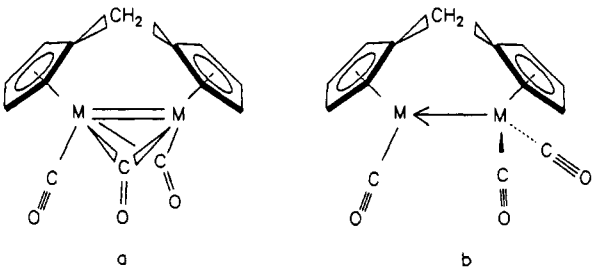

Figure 3. Possible intermediates in the side-to-side conversion of $CH_2[(\eta^5\text{-}C_5H_4)M(CO)]_2(\mu\text{-}CO)$ complexes.

Comparison of the $\Delta G^{\ddagger}$ values of the ring proton and carbonyl exchanges of I indicates that, within experimental error, both processes occur with the same energy barrier. This observation strongly suggests that these two exchanges occur in a concerted manner. While the requirement for simultaneity does not firmly establish the nature of the intermediates in this process, it does reduce the number of possibilities.

Lewis and his co-workers have proposed that the exchange of carbonyls in compounds of the general form, $(\eta^5\text{-}C_5H_5)_2M_2(CO)_{3-n}L_n$, may occur through a triply bridged intermediate, or through a synchronous exchange involving two carbonyls.[2,3] In the present examples, a triply bridged intermediate is precluded by the coupled rings, while processes involving the synchronous exchange of two carbonys appear quite reasonable. The two intermediates illustrated in Figure 3 are symmetric as would seem to be required by the coupling of the ring and bridge carbonyl motions. In one, Figure 3a, two bridging carbonyls form in the intermediate, while in the second, Figure 3b, the bridging carbonyl shifts to one metal, forming an all terminal species in which the metals are bound by a dative bond. Several examples of compounds of the general form $(\eta^5\text{-}C_5H_5)_2Rh_2(\mu\text{-}CO)_2L$, where R = H, CH_3, and L = phosphines, have been prepared and molecular structures of two representatives of this class of compounds have been reported.[11,12]

The energetics of the structural inversion and carbonyl exchange processes for several structurally related compounds are now available. Lewis and his co-workers found that the carbonyl exchange in *trans*-$(\eta^5\text{-}C_5H_5)_2Rh_2(CO)_3$ had $\Delta G^{\ddagger}$ values of 41.4 kJ/mol and 40.2 kJ/mol for the terminal and bridging carbonyls, respectively.[2,3] The higher values, 54.3 kJ/mol and 56.1 kJ/mol, respectively, found for I in this work probably reflects an increase in "stiffness" which results from the coupling of the cyclopentadienyl rings. The four-carbon bridge in $(CH_2CO)_2[(\eta^5\text{-}C_5H_4)Rh(CO)]_2(\mu\text{-}CO)$ has been found to raise the inversion barrier to about 58 kJ/mol, but the two carbonyl bridge in the recently prepared $(CH_2)_2[(\eta^5\text{-}C_5H_4)Rh(CO)]_2(\mu\text{-}CO)$ seems to substantially drop the barrier, such that it has not yet proved possible to freeze out the fluxional behavior of this compound even at temperatures of −50 °C. Studies of additional ring-bridged systems are currently underway to clarify these trends.

Comparison of the $\Delta G^{\ddagger}$ values for I and II indicate that substitution of iridium for rhodium results in a substantially increased inversion barrier. Since the molecular

(8) Kost, D.; Carlson, E. H.; Raban, M. *J. Chem. Soc., Chem. Comm.* **1971**, 656.
(9) Shanan-Atidi, H.; Bar-Eli, K. H. *J. Phys. Chem.* **1970**, *74*, 961.
(10) Sandström, J. *Dynamic NMR Spectroscopy*; Academic Press: New York, 1982.
(11) Farone, F.; Bruno, G.; Schiavo, S. L.; Piraino, P.; Bombieri, G. *J. Chem. Soc., Dalton Trans.* **1983**, 1819.
(12) Werner, H.; Klingert, B.; Zolk, R.; Thometzek, P. *J. Organometal. Chem.* **1984**, *266*, 97.

structures of I and II are effectively identical, there is no obvious structural reason for this difference in behavior. The root causes are probably related to the well-known increase in M–M and M–C bond strengths in going from the second to the third row transition elements which is reflected in the generally enhanced stability of compounds of the third row metals.

Experimental Section

General Considerations. $CH_2[(\eta^5\text{-}C_5H_4)Ir(CO)_2]_2$ was prepared by using a modification of the previously reported procedure in which $[IrCl(CO)_2(p\text{-toluidine})]$[13] is used as an iridium source rather than $[Ir(CO)_3Cl]_n$. I was prepared as previously reported. ^{13}CO was purchased from Aldrich. All reactions and NMR sample preparation were carried out under argon.

Infrared spectra were recorded on a Perkin Elmer 1750 FT-IR. Mass spectra were carried out by Dr. Gary Knerr of the University of Idaho using a VG 7070-HS GC/MS. NMR spectra were recorded on a Brucker WP 80 SY spectrometer (Padova) or an IBM 300-MHz FT-NMR spectrometer (Idaho). The proton spectral parameters were obtained by computer simulation of the experimental data on an Aspect-2000 Brucker computer with the Brucker PANIC program. Elemental analyses were conducted by Desert Analytics of Tucson, AZ.

Synthesis of $CH_2[(\eta^5\text{-}C_5H_4)Ir(CO)]_2(\mu\text{-}CO)$, II. $CH_2[(\eta^5\text{-}C_5H_4)IR(CO)_2]_2$, 250 mg (0.41 mmol), was placed in a 100-mL Schlenk flask outfitted with a condenser and a spin bar. Benzene, 50 mL, was added followed by an excess of Me_3NO, 0.50 g. The reaction mixture was refluxed for 6 h after which the solvent was removed by rotary evaporator and the resulting mixture chromatographed on neutral alumina with 1:1 dichloromethane–petroleum ether used as an elutant. An initial brown band consisting of a small amount of unreacted iridium starting material was rapidly eluted, followed by an orange band which was stripped of solvent to give 200 mg of II as an orange microcrystalline solid: mp 246–248 °C; yield 84%. IR: (CH_2Cl_2) 2002 (s), 1959 (w), 1776 (m). ^{13}C NMR: (CD_2Cl_2) 203.43 (μ-CO), 171.40 (terminal CO), 93.10 (ipso Cp), 87.80 (Cp), 87.21 (Cp), 86.94 (Cp), 84.44 (Cp), 6.09 (CH_2). Mass spectroscopy (electron impact): m/e 610 (72) M^+, 582 (39) $M^+ - CO$, 554 (100) $M^+ - 2CO$, 526 (51) $M^+ - 3CO$, 254 (62). Anal. Found: C, 27.62; H, 1.60. Calcd. for $C_{14}H_{10}Ir_2O_3$: C, 27.52; H, 1.62.

Synthesis of ^{13}CO-Labeled $CH_2[(\eta^5\text{-}C_5H_4)Rh(CO)]_2(\mu\text{-}CO)$, I. $CH_2[(\eta^5\text{-}C_5H_4)Rh(CO)]_2(\mu\text{-}CO)$, 250 mg (0.579 mmol), and benzene, 100 mL, were placed in a 500-mL Whitey stainless steel cylinder equipped with an inlet valve and a 1900 PSI safety rupture disk. The cylinder was immersed in a dry ice–2-propanol bath until its contents were frozen, and then the cylinder was evacuated and backfilled with ^{13}CO to 5 PSI. The cylinder was then closed off and immersed in a water bath (50 °C) for 2 days. After carefully venting the cylinder, the contents were transferred to a round-bottom flask and the solvent was removed. The resulting brown oil was chromatographed on alumina with petroleum ether to give $CH_2[(\eta^5\text{-}C_5H_4)Rh(CO)_2]_2$, which was characterized by IR, and a trace of $CH_2[(\eta^5\text{-}C_5H_4)Rh(CO)]_2(\mu\text{-}CO)$. After removal of the solvent, the $CH_2[(\eta^5\text{-}C_5H_4)Rh(CO)_2]_2$ was taken up in benzene and refluxed for 2 days, the solvent removed, and the resulting solid chromatographed on alumina with 1:1 dichloromethane–petroleum ether to give a single red-orange band. Removal of solvent gave 200 mg of I as a red solid. ^{13}C NMR: ($CDCl_3$) 232.53 (t, J_{Rh-C} = 46 Hz), 190.18 (d, J_{Rh-C} = 84 Hz), 93.61 (ipso C), 92.09 (Cp), 91.47 (Cp), 90.10 (Cp) (d, J_{Rh-C} = 4 Hz), 89.20 (Cp), 26.71 (CH_2). Yield: 88%.

X-ray Data Collection, Structure Determination, and Refinement for II. A single crystal of II (0.02 × 0.02 × 0.04 mm) was mounted on a Philips PW 1100 computer-controlled four-circle diffractometer with a graphite monochromator. Standard centering and autoindexing procedures[14] indicated a *primitive* orthorhombic lattice, space group *Pcmn*. The orientation matrix and accurate unit cell dimensions were determined from a least-square fit of 2*S* symmetry-related reflections ($16° < 2\theta < 30°$). Intensity data were collected at 24 °C by using the $\theta - 2\theta$ scan method; two standard reflections, monitored every 150 measurements, fluctuated within ±2% of their mean value. The intensities were corrected for Lorentz and polarization factors, but not for absorption, and scaled to give 1239 $F(hkl)$ values for which I was greater than $3(I)$. A summary of data collection parameters is given in Table I. Initial atom positions of I as reported by Werner et al.[5] were used, and subsequently refined with anisotropic thermal parameters (V_{ij}). Least-square calculations converged to the conventional R index of 0.081. The weighting scheme used in final calculations was with $w = 1$. Scattering factors for carbon and oxygen atoms were taken from Cromer and Waber[15] while those for Ir were taken from ref 16.

All computations were carried out on an IBM 758 computer with the program SHELX-76. The positional parameters of the atoms are listed in Table II in accord with the labeling scheme of Figure 1. Thermal parameters and the list of the structural factors are deposited in the supplementary material.

Acknowledgment. This work was supported in part by the National Research Council (CNR) through its Centro di Studio sugli Stati Molecolari Radicalici ed Eccitati and by the U.S. Naval Academy Research Council. T.E.B. gratefully acknowledges the travel support provided by the Faculty Development Fund of the U.S. Naval Academy and the generous support of the University of Idaho. We wish to thank Prof. Alan Balch for suggesting the use of $[Ir(CO)_2(p\text{-toluidene})]$ as a reagent for the synthesis of iridium carbonyl compounds. We also thank Prof. Jack Norton for his valuable suggestions concerning calculation of the carbonyl exchange barriers. The rhodium and iridium used in this research were the generous gifts of the Johnson Matthey Co.

Supplementary Material Available: Table of thermal parameters for II (1 page); a listing of observed and calculated structure factors (8 pages). Ordering information is given on any current masthead page.

(13) Klabunde, U. *Inorg. Synth.* **1974**, *15*, 82.

(14) Sparks, R. A. *Crystallographic Computing Techniques*; Ahmed, F. R. Ed.; Munksgaard: Copenhagen, 1976; p 452.

(15) Cromer, D. T.; Waber, J. T. *Acta Crystallogr.* **1965**, *18*, 104.

(16) *International Tables for X-Ray Crystallography*; Kynoch Press: Birmingham, U.K., 1974; Vol. IV.